

Infrared second harmonic generation spectroscopy of Ge(111) interfaces

D. Bodlakj,^{a)} E. Freysz,^{b)} and E. Borguet^{c)}

*Department of Chemistry and Surface Science Center, University of Pittsburgh,
Pittsburgh, Pennsylvania 15260*

(Received 9 December 2002; accepted 9 April 2003)

Infrared second harmonic generation (IR-SHG) spectroscopy, an extension of spectroscopic SHG to the IR, is described and applied to the investigation of germanium–dielectric interfaces in the spectral region near the direct and indirect band gap of the bulk semiconductor. The spectrum of the Ge(111)–GeO₂ interface, in the 1100–2000 nm fundamental wavelength range, is dominated by a resonance at 590 nm. This feature is assigned to the direct $\Gamma_{25'} > \Gamma_2$ transition between valence and conduction band states. Polarization and azimuth dependent IR-SHG spectroscopy revealed that the anisotropic contribution, containing bulk quadrupole, ξ , and surface, ∂_{11} , nonlinear susceptibility terms, dominates the 590 nm resonance. S-termination of Ge(111) significantly modifies the interface nonlinear optical response. The IR-SHG spectrum of S–Ge(111) presents a new, possibly surface resonance at ~ 565 nm, in addition to the resonance inherent to the bulk Ge at 590 nm, tentatively assigned to an interband transition of Ge atoms associated with the surface. © 2003 American Institute of Physics. [DOI: 10.1063/1.1578619]

INTRODUCTION

The first semiconductor transistor was based on germanium.¹ The initial preference for germanium was due to its superior carrier transport properties—the mobility of holes and electrons in Ge are more than twice those of Si.² Silicon, nevertheless, ultimately prevailed because the native oxide of germanium, GeO₂, does not form a stable interface with the semiconductor and is characterized by a higher trap/surface state density.³ Interest in Ge has renewed because of its use in high speed bipolar transistors and the ease with which it can be integrated with Si-based devices to fabricate emitters, modulators and receivers for optical communications, e.g., Ge-on-Si near-IR photodetectors.^{4,5}

Of the many spectroscopic techniques used to study chemically modified semiconductor surfaces, SHG studies are of particular interest since they provide surface sensitivity, probe the electronic response of the interface and can be carried out *in situ*.^{6–8} SHG can probe buried interfaces that are difficult to probe by conventional spectroscopic methods.⁹ The applicability of SHG to monitor charge, strain, microroughness as well as the progress of chemical reactions on semiconductor interfaces has been demonstrated.^{10–15} Germanium was one of the first semiconductors to be investigated by surface SHG.^{16–19} While the earliest experiments,¹⁶ did not report anisotropy in the SHG response with respect to rotation around the azimuthal axis (SHG-RA), later work revealed the presence of strong anisotropy.¹⁷ Si and Si_{1–x}Ge_x surfaces have been extensively studied

by SHG spectroscopy and rotational anisotropy but less attention was paid to germanium interfaces.^{6,12,20–23} Recently, Ohashi *et al.* reported the SHG spectrum of Ge–oxide interface in the 1.1–1.6 eV region and a surface resonance at 1.16 eV.²⁴

A detailed phenomenological theory of SHG-RA was developed and provides a framework for our understanding.^{25–28} The SHG response in the p_{in}/p_{out} polarization combination is described by

$$\begin{aligned} \frac{I_{pp}(2\omega)}{(I_p(\omega))^2} &\sim |A_{pp} + B_{pp} \cos(3\phi)|^2 \\ &= |A_{pp}|^2 + |B_{pp}|^2 \cos^2(3\phi) \\ &\quad + 2|A_{pp}|^* |B_{pp}| \cos(3\phi) \cos(\Delta_{AB}), \end{aligned} \quad (1)$$

where ϕ is the azimuthal angle measured between the plane of incidence and the $[2\bar{1}\bar{1}]$ direction of the single crystal.²⁹ A_{pp} , the isotropic contribution and B_{pp} , the anisotropic contribution are specific to the p_{in}/p_{out} polarization combination. They depend on the nonlinear coefficients, angle of incidence and the linear optical properties of the interface at the fundamental and second harmonic wavelengths.²⁹ A_{pp} and B_{pp} are complex, having a relative phase Δ_{AB}

$$\frac{A_{pp}}{B_{pp}} = \left| \frac{A_{pp}}{B_{pp}} \right| \exp(i\Delta_{AB}). \quad (2)$$

A_{pp} and B_{pp} are related to the microscopic nonlinear susceptibility elements by

$$\begin{aligned} A_{pp} &= A_p \left[a_{1pp} \xi + a_{2pp} \left(\frac{\gamma}{\epsilon(2\omega)} + \partial_{31} \right) \right. \\ &\quad \left. + a_{3pp} (\partial_{31} - \partial_{33}) + a_{4pp} \partial_{15} \right], \end{aligned} \quad (3)$$

$$B_{pp} = A_p [b_{1pp} \xi + b_{2pp} \partial_{11}], \quad (4)$$

^{a)}Present address: Department of Chemistry, University of Wisconsin, Madison.

^{b)}Permanent address: Center de Physique Moléculaire Optique et Hertzienne, Université de Bordeaux 1, 351 Cours de la Libération, 33405 Talence, Cedex, France.

^{c)}Author to whom correspondence should be addressed. Electronic mail: borguet@pitt.edu

The nonlinear susceptibility elements $\partial_{11}, \partial_{15}, \partial_{31}, \partial_{33}$ describe the electric-dipole response of the surface. ∂_{11} contributes to the anisotropic response (B_{pp}). $\partial_{15}, \partial_{31}$, and ∂_{33} determine the isotropic response (A_{pp}) of the SHG signal. A_{pp} and B_{pp} have bulk electric-quadrupole contributions, described by the bulk nonlinear susceptibilities γ and ξ . The a and b coefficients as well as A_p in Eqs. (3) and (4), depend only on the linear dielectric parameters of the interface and the angle of incidence.²⁹ The s -polarized SHG signal has only anisotropic contributions and is given by the following expression:

$$\frac{I_{ps}(2\omega)}{(I_p(\omega))^2} \sim |B_{ps} \sin(3\phi)|^2. \quad (5)$$

SHG spectroscopy has been successfully applied to semiconductor/oxide surfaces in the visible.^{21–23} However, the region near the bandgap of Si and Ge, that lies in the IR, has not been probed. IR+VIS SFG is the traditional approach to probing resonances in the IR spectral region. We propose IR-SHG as an alternative. The IR-SHG approach has the advantage of probing resonances that exist solely at the fundamental or second harmonic photon energies. IR-SHG overcomes several potential limitations of IR+VIS SFG, namely the much larger nonlinear optical response that can occur at SF or VIS wavelengths, e.g., for metal and semiconductor interfaces. The nonresonant response can obscure the smaller resonant response at IR wavelengths, as is expected to be the case for infragap states when the sum frequency and/or visible wavelengths are resonant with supragap states in semiconductors. In addition, the intense visible photon source can perturb the interface response by electron–hole pair generation, or induce an EFISH response by multiphoton charging of the interfacial dielectric.³⁰ For example, recently, doubly resonant IR+VIS SFG, a technique that gives access to information about the electron–vibration coupling of surface molecules was demonstrated experimentally.³¹ While these phenomena may be of interest themselves, it is also useful to study the interface response in the absence of these couplings. The surface SHG response has not been probed previously beyond 1530 nm, for a number of reasons: Lack of detectors with single photon counting capabilities at IR wavelengths, and a lack of intense IR sources.³²

We have used our short pulse (1 to 2 ps) narrowband ($<15 \text{ cm}^{-1}$), tunable optical parametric amplifier (OPA),³³ coupled with the near-IR single photon counting capabilities of Si CCD devices, to extend SHG spectroscopy to the IR. The present work focuses on the influence of the chemical state of the surface on the nonlinear optical spectroscopy of Ge–GeO₂ and Ge–S interfaces. The 1100–2000 nm fundamental photon wavelength range explored includes the direct and indirect gaps of germanium.

EXPERIMENT

Sample preparation

Ge(111) wafers (undoped, Eagle Picher) were degreased by successive 10-minute sonications in trichloroethylene (J.T. Baker reagent grade), acetone (EM Science, reagent grade), then methanol (Fisher Scientific, Certified ACS

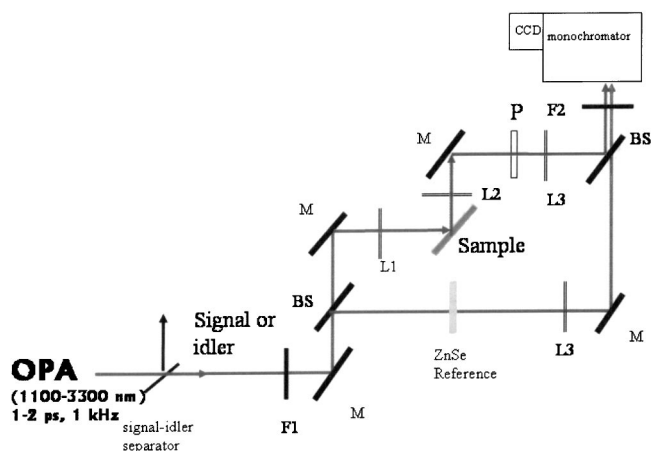


FIG. 1. IR-SHG experimental setup. The output of OPA (40 μJ , 1.1–3.3 μm , 1 to 2 ps, 1 kHz) is filtered (signal-idler separator and F1) and focused onto the sample (L1). Second harmonic generated at sample is collimated (L2), polarized (P), filtered (F2) and focused to monochromator (L3). Signal is detected by CCD camera, in single element mode. ZnSe is used as a reference.

grade). No additional treatment was performed on oxidized samples before experiments. All chemicals were purchased from Aldrich Co., unless otherwise stated, and used as received. The clean, oxidized Ge samples were hydrogen terminated by dipping in 48% HF (Mallinckrodt, reagent grade) five times for 10 s, each time followed by a 20 s rinse in nanopure water. Finally, the sample was dried in N₂ gas.³⁴ Sulfidation of the Ge(111) surface was achieved by immersion of hydrogen terminated Ge in (NH₄)₂S at 70 °C for 20 min followed by rinsing in methanol and drying by N₂ flow.^{35,36}

Infrared second harmonic generation spectroscopy

The setup for IR-SHG spectroscopic studies is depicted in Fig. 1. To cover the 1100–2000 nm range both signal and idler wavelengths of the OPA were used.³³ The OPA was used in a 3 KTP crystal configuration to increase the wavelength range and overall power of the output ($>40 \mu\text{J}/\text{pulse}$). The IR output of the OPA was spectrally filtered to remove second harmonic photons, and divided into a reference and sample arm. The reference arm consisted of a ZnSe crystal as source of second harmonic generation. ZnSe is transparent over the wavelength range scanned. In the absence of an optical resonance, any second harmonic intensity change should only contain information about variation in laser source parameters. The sample arm contained the sample with appropriate focusing and collimating lenses before and after the sample. The OPA output was strongly polarized and could be changed from p to s at the sample by use of a periscope. The spot size on the sample was about 10^{-4} cm^2 . The beam area was corrected for the elliptical shape obtained at non-normal incidence. The second harmonic signal, reflected off the sample, was collected by the collimating lens, and then focused onto the monochromator entrance slit (Acton Research, 300 gr/mm grating). An analyzing polarizer was set to pass either s - or p -polarized SHG photons, after short pass filtering to block IR photons. The quadratic nature

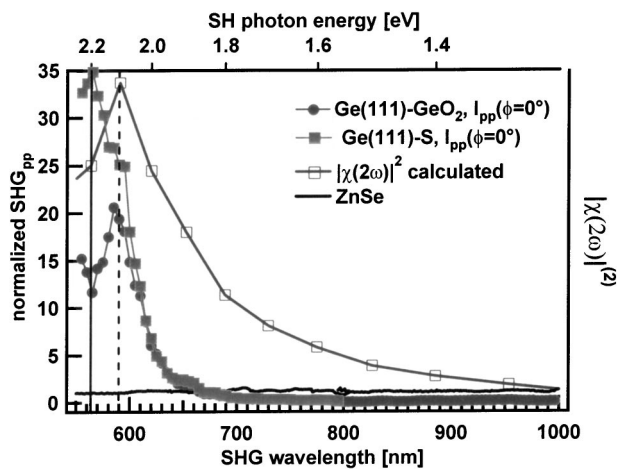


FIG. 2. IR-SHG spectra of Ge(111)-GeO₂ (●) and Ge(111)-S (■) interfaces. The spectra were taken in the p_{in}/p_{out} polarization combination at $\phi=0^\circ$. The second-order nonlinear response calculated from the linear properties of germanium is also shown (□). The dashed vertical lines indicate the resonance at 590 nm. The solid vertical line indicates the resonance at 565 nm.

of second harmonic response was verified in the power range explored.³⁷ The signal was detected by a 1024×256 pixel, liquid nitrogen cooled CCD camera (Princeton Instrument, CCD30-11). Selected regions of the CCD chip were defined as detection areas for SHG signals from the sample and reference, and recorded simultaneously as the OPA was scanned, in 5 nm/step increments, over the entire wavelength range. The normalized SHG, i.e., the ratio of the sample and reference signals, is reported. Consecutive scans were taken and, if necessary, several scans were averaged. Typically, scans were reproducible to within 5% and no averaging was required. Depending on the sample signal levels, acquisition times were 4–10 s per step. The spectral range is limited at shorter wavelength ($\lambda_{2\omega}=560$ nm) due to low OPA power and consequently low SHG signal levels. The long wavelength limit, $\lambda_{\omega}\sim 2100$ nm, is set by the CCD spectral response. Second harmonic generation rotational anisotropy (SHG-RA) measurements were carried out to control the exactness of the crystal cut and the effects of wet chemical treatment.²⁹

RESULTS AND DISCUSSION

The IR-SHG spectrum of Ge-GeO₂ interface in the 1100–2000 nm fundamental (NIR) wavelength range in the p_{in}/p_{out} polarization is shown in Fig. 2 (filled circles). The $\chi^{(2)}$ in the p_{in}/p_{out} polarization combination contains all the nonzero surface nonlinear susceptibility components (i.e., $\partial_{31}, \partial_{33}, \partial_{15}, \partial_{11}$ surface electric dipole components and ξ, γ bulk quadrupole components). At the 0° azimuth both A_{pp} and B_{pp} are active [Eq. (1)]. The characteristic feature of the spectrum is the peak in SHG at a fundamental wavelength of 1180 nm (590 nm SHG). For comparison, the spectrum of the reference ZnSe sample, taken by replacing Ge with a ZnSe in the sample arm, is plotted on Fig. 2 (solid line). The spectrum of ZnSe, taken as baseline for the measurement, is flat in scanned wavelength range, showing <10% standard deviation.

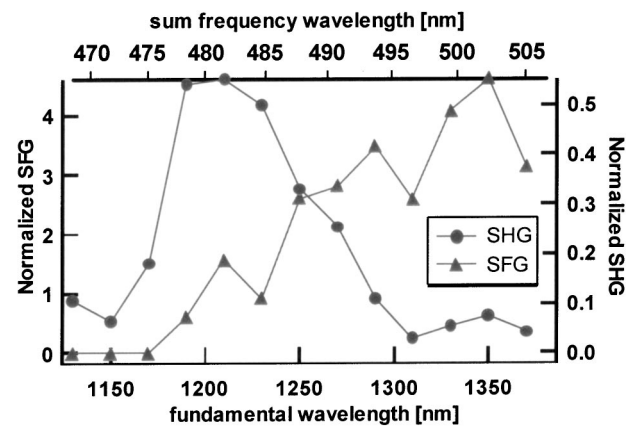


FIG. 3. IR-SHG and SFG (IR+800 nm) spectra of Ge(111)-GeO₂. The IR-SHG spectrum (●) and SFG spectrum (▲) were taken in the p_{in}/p_{out} polarization combination at $\phi=0^\circ$.

The second harmonic response can be estimated from the bulk optical properties of germanium based on

$$\chi(2\omega) = \varepsilon(2\omega) - 1, \quad (6)$$

where $\chi(2\omega)$ is the second-order susceptibility, $\varepsilon(2\omega)$ is the dielectric constant at the SHG frequency.¹² The measured SHG response in Fig. 2 (filled circles) follows the predicted trend (open squares) qualitatively, so we attributed the enhancement in the second harmonic signal to the direct $\Gamma_{25} > \Gamma_2$ transition between the valence and conduction band states.^{38,39} The indirect band gap of germanium is at 1878 nm (0.66 eV), the direct band gap is at 1670 nm (0.74 eV).⁴⁰ No strong resonances are observed at either the indirect ($\lambda_{2\omega}=939$ nm) or direct band edges ($\lambda_{2\omega}=835$ nm) gaps. Indeed, the SHG response appears more sharply peaked than might be expected from the linear optical properties alone.

The sum frequency generation spectrum, i.e., mixing of the 800 nm and signal (1100–1600 nm) photons was taken to test whether the resonance is at the second harmonic or at the fundamental wavelength (Fig. 3). The IR-SHG spectrum shows the resonant feature at ~ 1180 nm. In contrast, the SFG signal increases steadily with increasing fundamental wavelength. The absence of the resonance at 1180 nm in the SFG spectrum suggests that there is no resonance at the fundamental IR wavelength. Thus, a resonance at the SHG wavelength (590 nm, 2.1 eV) must be responsible for the peak in the SHG spectrum.

With the proper choice of the polarization of the incident fundamental and the SHG photons and the azimuthal angle of the Ge(111) sample, the dispersion of the isotropic and anisotropic contribution can be probed individually. The p_{in}/p_{out} , and p_{in}/s_{out} rotational anisotropy patterns, Fig. 4, show threefold symmetry with three small and three large peaks separated by 120° with no isotropic offset above the background. Rotating the sample to the $\phi=30^\circ$ azimuth in the p_{in}/p_{out} polarization combination turns off the anisotropic contribution B_{pp} and only A_{pp} is probed [Fig. 4(a)].

The IR-SHG spectrum of the Ge(111)-GeO₂ interface recorded in the p_{in}/p_{out} polarization combination at $\phi=0^\circ$, Fig. 2, probes both A_{pp} , and B_{pp} . B_{pp} alone cannot be probed in the p_{in}/p_{out} polarization combination but can be

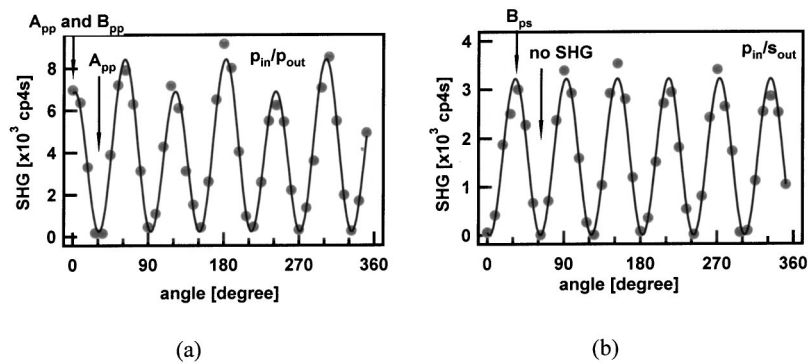


FIG. 4. SHG-RA of Ge(111)–GeO₂ at 1380 nm fundamental wavelength. (a) SHG-RA in the p_{in}/p_{out} polarization combination. (b) SHG-RA in the p_{in}/s_{out} polarization combination. The isotropic and anisotropic components probed at the various azimuths are shown by arrows.

investigated in the p_{in}/s_{out} polarization combination [Fig. 4(b)]. The anisotropic component, B_{ps} , of the p_{in}/s_{out} polarization combination contains the same, bulk quadrupole ξ , and surface, ∂_{11} , nonlinear susceptibility terms as B_{pp} .²⁹ The p_{in}/s_{out} polarization combination only comprises an anisotropic term. Therefore, at $\phi=0^\circ$ no p_{in}/s_{out} second harmonic signal should be generated. It is clear that by a judicious choice of polarizations and sample orientation, the individual isotropic and anisotropic components can be probed.

The IR-SHG spectrum of the Ge(111)–GeO₂ interface was taken in the 1100–1600 nm range with an appropriate choice of polarization combination so that both isotropic, A_{pp} , and anisotropic B_{pp} , only the isotropic, A_{pp} , and only the anisotropic, B_{ps} , contributions were sampled, respectively (Fig. 5). There is a resonance at 590 nm in the spectrum of the anisotropic, B_{ps} , contribution, which coincides with the resonance observed when both the isotropic, A_{pp} , and anisotropic, B_{pp} , components were probed. The resonance at 590 nm was assigned to the direct $\Gamma_{25} > \Gamma_2$ transition between valence and conduction band states.³⁹ The association of the resonance with B_{pp} but not A_{pp} , indicates that the interband transition affects mainly the ξ and/or ∂_{11} nonlinear susceptibility components. In contrast, A_{pp} shows no peak but increases steadily as the wavelength decreases.

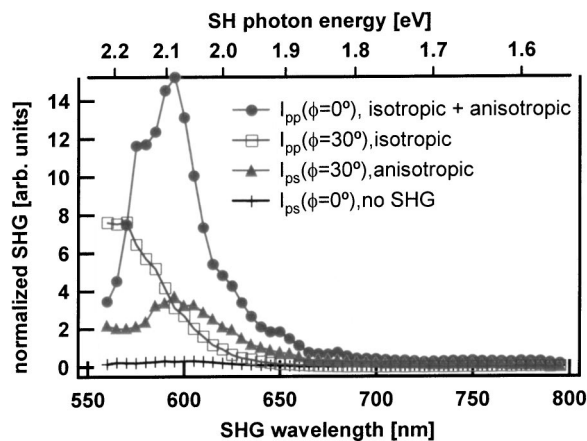


FIG. 5. IR-SHG spectrum of Ge(111)–GeO₂ in the 1100–1600 nm range. Both A_{pp} and B_{pp} components are probed in p_{in}/p_{out} polarization at $\phi=0^\circ$ (●). The isotropic, A_{pp} , component is probed in the p_{in}/p_{out} polarization combination at $\phi=30^\circ$ (□). B_{ps} is probed in the p_{in}/s_{out} polarization combination at $\phi=30^\circ$ (▲). At $\phi=0^\circ$ in the p_{in}/s_{out} polarization combination no SHG was generated (+).

The spectrum of A_{pp} is suggestive of a peak at shorter wavelength outside our experimental range. The increase of A_{pp} , while the SHG decreases when both A_{pp} and B_{pp} , is probed indicates that A_{pp} and B_{pp} are out of phase at <590 nm. This is consistent with a resonance in one component B_{pp} , but not the other A_{pp} , at 590 nm.

The linear optical properties of Ge can be used to predict possible SHG resonances at shorter wavelength [Eq. (6)].²² The bulk spectrum of Si_{1-x}Ge_x is characterized by direct interband transitions, E'_0/E_1 and E_2 in the 2–5 eV range.⁴¹ In Si they occur at 3.3 and 4.2 eV, respectively.^{38,39} Daum *et al.* recorded the SHG spectra of the Si(100)–SiO₂ interface in the 3.2–4.4 eV (388–282 nm) range.²² The direct bulk interband transitions, E'_0/E_1 and E_2 were at 3.3 and 4.2 eV were identified.²² A strong transition at 3.6 eV was also found that had no equivalent in the bulk of the crystalline Si. The 3.6 eV feature was attributed to the unique bonding configuration of Si atoms at the interface.²² Such surface resonance can be expected at the Ge(111)–GeO₂ interface between 2.1 and 4.2 eV. The peak at 4.2 eV does not disperse as the Ge content increases, whereas the peak at 3.3 eV redshifts to lower energy as the Ge content increases.⁴¹ For pure Ge it lies at 2.1 eV.

Chemical termination, and the changes to the SHG response, can be used as a basis for separating the contributions of the surface and the bulk.²⁹ Surface functionalization should change mainly the surface properties while leaving the bulk response intact. Recently, a number of routes to air stable termination/passivation layers of germanium have been reported. Notably, wet chemical preparation of H-, Cl-, S-, and alkyl-terminations of Ge(111) and Ge(100) have been described.^{34–36,42–45} Combined SHG and XPS experiments have shown that H- and Cl-terminated surfaces rapidly oxidize in ambient, while S- and alkyl-terminations are stable for weeks.⁴⁶ Sulfidation of the Ge(111) surface was used here to test the surface character of the transition observed at 590 nm (2.1 eV). The IR-SHG spectra of Ge(111)–GeO₂ and Ge(111)–S in the 1100–1600 nm fundamental wavelength range are shown in Fig. 2. The resonance at 590 nm, attributed to the direct $\Gamma_{25} > \Gamma_2$ transition between valence and conduction band states, is present in the Ge(111)–S spectrum as a shoulder.⁴⁰ However, the dominant feature in the Ge(111)–S spectra is the peak at shorter wavelength, ~ 565 nm. This peak is absent in the IR-SHG spectra of the Ge(111)–GeO₂ interface. Clearly, the resonance at the

<565 nm is the result of the surface modification, i.e., sulfide termination.

The apparent peak at 565 nm is most likely of surface origin especially since it is the result of the S-termination. Therefore, we assign the peak at \sim 565 nm to an interband transition of Ge atoms associated with the surface. The surface origin of the peak at 565 nm is further confirmed by a recent report of a resonance at 1070 nm (1.16 eV) fundamental wavelength.²⁴ The resonance was present in the SHG spectrum of the Ge(111)-thermal oxide interface only but not at the Ge(111)-native oxide interface indicating its surface origin.²⁴ The close proximity of the resonance reported here, i.e., 565 nm versus 535 nm SH wavelength, suggests that we observed the same resonance but redshifted at the Ge(111)-S interface. Furthermore, Lyman *et al.* found that passivation of Ge(001) in (NH₄)₂S (24% in H₂O) results in 2.4 ML S coverage.³⁶ The overlayer was described as a disordered (glasslike) GeS_x layer residing atop a partially ordered interfacial layer.³⁶ The authors pointed out that their model is reminiscent of the often-proposed picture of the intensely studied Si-SiO₂ interface; a partially ordered interfacial SiO_x whose order breaks down for SiO₂ layers more than several angstrom thick.³⁶ It is interesting to note that the IR-SHG spectrum of the Ge(111)-S interface is similar to the SHG spectrum of Si(100)-SiO₂ interface as the resonance of surface origin lies between the bulk interband transitions of Ge, i.e., between 2.1 and 4.2 eV.²²

CONCLUSIONS

We have extended surface SHG spectroscopy into the IR; infrared second harmonic generation (IR-SHG), and applied it to the investigation of germanium-dielectric interfaces in the spectral region near the direct and indirect band gaps of the bulk semiconductor. The spectrum of the Ge(111)-GeO₂ interface, in the 1100-2000 nm fundamental wavelength range, is dominated by a resonance at 590 nm. This feature is assigned to the direct $\Gamma_{25}' > \Gamma_2$ transition between valence and conduction band states. Polarization and azimuth dependent IR-SHG spectroscopy revealed that the anisotropic contribution, containing bulk quadrupole, ξ , and surface, ∂_{11} , nonlinear susceptibility terms, contributes mostly to the 590 nm resonance. S-termination of Ge(111) significantly modifies the interface nonlinear optical response. The IR-SHG spectrum of S-Ge(111) presents a new, possibly surface resonance, at \sim 565 nm in addition to the resonance inherent to the bulk Ge at 590 nm. This resonance is assigned to an interband transition associated with the surface Ge atoms.

ACKNOWLEDGMENTS

The authors acknowledge the generous support of the NSF (CHE-9734273). E.B. acknowledges the NSF for a CAREER award in support of this research.

¹J. Bardeen and W. H. Brattain, Phys. Rev. **74**, 230 (1948).

²C. Kittel, *Introduction to Solid State Physics*, 6th ed. (Wiley, New York, 1986).

³P. Balk, in *The Si-SiO₂ System*, edited by P. Balk (Elsevier, Amsterdam, 1988), Vol. 32, pp. 2-20.

- ⁴J. Oh, J. C. Campbell, S. G. Thomas, S. Bharatan, R. Thoma, C. Jasper, R. E. Jones, and T. E. Zirkle, IEEE J. Quantum Electron. **38**, 1238 (2002).
- ⁵E. Maruyama, S. Okamoto, A. Terakawa, W. Shinohara, M. Tanaka, and S. Kiyama, Sol. Energy Mater. Sol. Cells **74**, 339 (2002).
- ⁶H. W. K. Tom, T. F. Heinz, and Y. R. Shen, Phys. Rev. Lett. **51**, 1983 (1983).
- ⁷Y. R. Shen, Nature (London) **337**, 519 (1989).
- ⁸T. F. Heinz, "Second-order nonlinear optical effects at surfaces and interfaces," in *Nonlinear Surface Electromagnetic Phenomena*, edited by H. E. Ponath and G. I. Stegeman (Elsevier Science, New York, 1991), p. 353.
- ⁹G. Lüpke, Surf. Sci. Rep. **35**, 75 (1999).
- ¹⁰J. I. Dadap, P. T. Wilson, M. H. Anderson, and M. C. Downer, Opt. Lett. **22**, 901 (1997).
- ¹¹J. Fang and G. P. Li, Appl. Phys. Lett. **75**, 3506 (1999).
- ¹²W. Daum, H. J. Krause, U. Reichel, and H. Ibach, Phys. Rev. Lett. **71**, 1234 (1993).
- ¹³J. I. Dadap, B. Doris, Q. Deng, M. C. Downer, J. K. Lowell, and A. C. Diebold, Appl. Phys. Lett. **64**, 2139 (1994).
- ¹⁴S. A. Mitchell, R. Boukherroub, and S. Anderson, J. Phys. Chem. B **104**, 7668 (2000).
- ¹⁵S. A. Mitchell, M. Mehendale, D. M. Villeneuve, and R. Boukherroub, Surf. Sci. **488**, 367 (2001).
- ¹⁶N. Bloembergen, R. K. Chang, S. S. Jha, and C. H. Lee, Phys. Rev. **174**, 813 (1968).
- ¹⁷D. Guidotti, T. A. Driscoll, and H. J. Gerritsen, Solid State Commun. **46**, 46 (1983).
- ¹⁸J. A. Litwin, J. E. Sipe, and H. M. Van Driel, Phys. Rev. B **31**, 5543 (1985).
- ¹⁹O. A. Aktsipetrov, I. M. Baranova, and Y. A. Il'inskii, Sov. Phys. JETP **64**, 167 (1986).
- ²⁰P. R. Fisher, J. L. Daschbach, and G. L. Richmond, Chem. Phys. Lett. **218**, 200 (1994).
- ²¹G. Erley, R. Butz, and W. Daum, Phys. Rev. B **59**, 2915 (1999).
- ²²G. Erley and W. Daum, Phys. Rev. B **58**, R1734 (1998).
- ²³P. S. Parkinson, D. Lim, R. Büngener, J. G. Ekerdt, and M. C. Downer, Appl. Phys. Lett. **68**, 641 (1999).
- ²⁴H. Ohashi, H. Sano, and G. Mizutani, Jpn. J. Appl. Phys. **40**, 6972 (2001).
- ²⁵O. A. Aktsipetrov, I. M. Baranova, and Y. A. Il'inskii, Zh. Eksp. Teor. Fiz. **91**, 287 (1986).
- ²⁶J. E. Sipe, D. L. Moss, and H. M. van Driel, Phys. Rev. B **35**, 1129 (1987).
- ²⁷V. Mizrahi, and J. E. Sipe, J. Opt. Soc. Am. B **5**, 660 (1988).
- ²⁸G. Lüpke, D. J. Bottomley, and H. M. van Driel, J. Opt. Soc. Am. B **11**, 33 (1994).
- ²⁹V. Fomenko, D. Bodlaki, C. Falser, and E. Borguet, J. Chem. Phys. **116**, 6745 (2002).
- ³⁰V. Fomenko, C. Hurth, T. Ye, and E. Borguet, J. Appl. Phys. **91**, 4394 (2002).
- ³¹M. B. Raschke, M. Hayashi, S. H. Lin, and Y. R. Shen, Chem. Phys. Lett. **359**, 367 (2002).
- ³²E. K. L. Wong, K. A. Friedrich, and G. L. Richmond, Chem. Phys. Lett. **195**, 628 (1992).
- ³³D. Bodlaki and E. Borguet, Rev. Sci. Instrum. **71**, 4050 (2000).
- ³⁴T. Deegan and G. Hughes, Appl. Surf. Sci. **123**, 66 (1998).
- ³⁵G. W. Anderson, M. C. Hanf, P. R. Norton, Z. H. Lu, and M. J. Graham, Appl. Phys. Lett. **66**, 1123 (1995).
- ³⁶P. F. Lyman, O. Sakata, D. L. Marasco, T. L. Lee, K. D. Breneman, D. T. Keane, and M. J. Bedzyk, Surf. Sci. **462**, L594 (2000).
- ³⁷V. Fomenko, J. F. Lami, and E. Borguet, Phys. Rev. B **63**, 121316 (2001).
- ³⁸*Handbook of Optical Constants of Solids*, edited by E. D. Palik (Academic, San Diego, 1998).
- ³⁹F. Wooten, *Optical Properties of Solids* (Academic, New York, 1972).
- ⁴⁰S. M. Sze, *Physics of Semiconductor Devices*, 2nd ed. (Wiley, New York, 1981).
- ⁴¹J. Humlicek, M. Garriga, M. I. Alonso, and M. Cardona, J. Appl. Phys. **65**, 2827 (1989).
- ⁴²Z. H. Lu, Appl. Phys. Lett. **68**, 520 (1996).
- ⁴³K. Choi and J. M. Buriak, Langmuir **16**, 7737 (2000).
- ⁴⁴S. M. Han, W. R. Ashurt, C. Carraro, and R. Maboudian, J. Am. Chem. Soc. **123**, 2422 (2001).
- ⁴⁵J. L. He, Z. H. Lu, S. A. Mitchell, and D. D. M. Wayner, J. Am. Chem. Soc. **120**, 2660 (1998).
- ⁴⁶D. Bodlaki, H. Yamamoto, D. H. Waldeck, and E. Borguet, Surf. Sci. (to be published).